Transactions Letters

Residual Frequency Offset Compensation Using the Approximate SAGE Algorithm for OFDM System

Jong-Ho Lee and Seong-Cheol Kim, *Member, IEEE*

***Abstract*—In this letter, we propose an iterative detection scheme in the presence of residual frequency offset (RFO) for orthogonal frequency-division multiplexing systems using an approximate application of the space-alternating generalized expectation-maximization (SAGE) algorithm. In the proposed scheme, the expectation step intends to divide the received signal into the desired signal and the interference signal. In the maximization step, the desired signal is used to estimate required parameters (i.e., RFO, data symbols, and channel state information) sequentially. Simulation results present that the proposed scheme shows almost ideal performance as long as the normalized RFO value is within 0.2.**

***Index Terms*—Carrier frequency offset (CFO), orthogonal frequency-division multiplexing (OFDM), space-alternating generalized expectation-maximization (SAGE).**

I. Introduction

ORTHOGONAL frequency-division multiplexing (OFDM) is an attractive technique to support high-rate data transmission over severely dispersed multipath fading channels. However, it is known that OFDM is very sensitive to carrier-frequency synchronization and channel-estimation errors [1].

Carrier frequency offset (CFO) due to the mismatch of the local oscillators in the transceiver causes intercarrier interference (ICI), which may result in significant performance degradation. Several carrier-frequency-synchronization schemes for OFDM systems are reported in the literature [2]–[6]. However, residual frequency offset (RFO) due to imperfect synchronization still generates ICI and severely degrades the transmission performance [7]. In order to estimate the RFO, [8] and [9] use virtual subcarriers that are not actually modulated, considering the orthogonality between subcarriers.

In this letter, we employ the space-alternating generalized expectation-maximization (SAGE) algorithm [10] to overcome the ICI due to the RFO. In the proposed scheme, the expectation step removes the ICI induced by the RFO in the received signals. Then, the maximization step estimates the RFO, data symbols, and channel state information (CSI).

Paper approved by C. Tepedelenlioglu, the Editor for Transmission Systems of the IEEE Communications Society. Manuscript received March 2, 2005; revised July 5, 2005; November 10, 2005; and November 17, 2005. This work was supported in part by the University IT Research Center Project and in part by the Brain Korea 21 Project.

J.-H. Lee was with the Institute of New Media and Communications, School of Electrical Engineering and Computer Science, Seoul National University, Seoul 151-742, Korea. He is now with Samsung Electronics, Seoul 100-742, Korea.

S.-C. Kim is with the Institute of New Media and Communications, School of Electrical Engineering and Computer Science, Seoul National University, Seoul 151-742, Korea (e-mail: sckim@maxwell.snu.ac.kr).

Digital Object Identifier 10.1109/TCOMM.2006.874014

II. System Model

Let N be the number of subcarriers and $N_s = 2N_\alpha + 1$ be the number of modulated subcarriers [11], [16]. Note that $N - N_s$ subcarriers at the edges of the spectrum are not used. Then the time-domain received signal vector $\mathbf{r} = [r(0)\ r(1)\ \cdots\ r(N-1)]^T$ over a frequency-selective fading channel can be written as

$$\mathbf{r} = \mathbf{F}_\upsilon \mathbf{FSDh} + \mathbf{w} \tag{1}$$

where the normalized RFO υ is presented in the matrix $\mathbf{F}_\upsilon$ given as

$$\mathbf{F}_\upsilon = \mathrm{diag}\left\{1, e^{j\frac{2\pi\upsilon}{N}}, \ldots, e^{j\frac{2\pi\upsilon}{N}(N-1)}\right\} \tag{2}$$

and the transmitted data symbols are given in the diagonal data symbol matrix

$$\mathbf{S} = \mathrm{diag}\left\{s_0, s_1, \ldots, s_{N_s-1}\right\}. \tag{3}$$

The subcarrier signals are shown in the matrix $\mathbf{F}$ with entries

$$[\mathbf{F}]_{n,p} = \frac{1}{\sqrt{N}} e^{j\frac{2\pi(p-N_\alpha)}{N}n} \tag{4}$$

where $n = 0, 1, \ldots, N-1$ and $p = 0, 1, \ldots, N_s - 1$. Moreover, the discrete Fourier transform (DFT) matrix $\mathbf{D}$ is given as $[\mathbf{D}]_{p,l} = e^{-j(2\pi(p-N_\alpha)/N)l}$ where $l = 0, 1, \ldots, L-1$. In (1), $\mathbf{h} = [h(0)\ h(1)\ \cdots\ h(L-1)]^T$ and $\mathbf{w} = [w(0)\ w(1)\ \cdots\ w(N-1)]^T$ denote the channel impulse response (CIR) with L multipaths and the additive white Gaussian noise (AWGN) vector, respectively.

III. Proposed Scheme

A. RFO Compensation via the SAGE Algorithm

The frequency-domain received signal vector can be represented as

$$\mathbf{z} = \mathbf{F}^H\mathbf{r} = \varepsilon\mathbf{SDh} + \mathbf{RSDh} + \mathbf{v} \tag{5}$$

where $(.)^H$ denotes the conjugated transpose and $\mathbf{v}$ has the covariance matrix of $\sigma^2\mathbf{I}$. It is seen that ε in (5) affects all the subcarriers constantly, and is given by

$$\varepsilon = \frac{1}{N}\sum_{n=0}^{N-1} e^{j\frac{2\pi\upsilon}{N}n}. \tag{6}$$

Here, we refer to ε as a common RFO error. In (6), assuming υ is sufficiently small and ε is given, we can obtain approximately using the Taylor's series expansion $(e^{j(2\pi\upsilon/N)n} \approx 1 + j(2\pi\upsilon/N)n)$ given as

$$\upsilon \approx \frac{N}{\pi(N-1)}\Im\{\varepsilon\}. \tag{7}$$

Moreover, $\mathbf{R}$ in (5) induces the ICI due to the RFO given by

$$\mathbf{R} = \mathbf{F}^H\mathbf{F}_\upsilon\mathbf{F} - \varepsilon\mathbf{I} \tag{8}$$

where its diagonal terms are equal to zero.

In the proposed scheme based on the SAGE algorithm, we intend to divide the received signal $\mathbf{z}$ in (5) into the desired signal

$$\mathbf{z}_D = \varepsilon\mathbf{SDh} + \beta_D\mathbf{v} \tag{9}$$

and the interference signal

$$\mathbf{z}_I = \mathbf{RSDh} + \beta_I\mathbf{v} \tag{10}$$

which indicates the transformation from the incomplete observation $\mathbf{z}$ to the complete observations $\mathbf{z}_D$ and $\mathbf{z}_I$ in the expectation-maximization (EM) algorithm, where $\beta_D^2 + \beta_I^2 = 1$ [12], [13]. A similar approach for the channel-estimation issue with transmitter diversity is also shown in [14]. Then, we try to estimate ε, $\mathbf{s} = [s_0\ s_1\ \cdots\ s_{N_s-1}]^T$ and $\mathbf{h}$ using the desired signal $\mathbf{z}_D$ in (9).

In the expectation step at the (k)th iteration, the following expectations are evaluated:

$$\begin{aligned}\mathbf{z}_D^{(k)} &= E\left[\mathbf{z}_D|\varepsilon^{(k)}, \mathbf{s}^{(k)}, \mathbf{h}^{(k)}, \mathbf{z}\right] \\ &= \varepsilon^{(k)}\mathbf{S}^{(k)}\mathbf{Dh}^{(k)} \\ &\quad + \beta_D^2\left(\mathbf{z} - \varepsilon^{(k)}\mathbf{S}^{(k)}\mathbf{Dh}^{(k)} - \mathbf{R}^{(k)}\mathbf{S}^{(k)}\mathbf{Dh}^{(k)}\right) \quad (11)\\ \mathbf{z}_I^{(k)} &= E\left[\mathbf{z}_I|\varepsilon^{(k)}, \mathbf{s}^{(k)}, \mathbf{h}^{(k)}, \mathbf{z}\right] \\ &= \mathbf{R}^{(k)}\mathbf{S}^{(k)}\mathbf{Dh}^{(k)} \\ &\quad + \beta_I^2\left(\mathbf{z} - \varepsilon^{(k)}\mathbf{S}^{(k)}\mathbf{Dh}^{(k)} - \mathbf{R}^{(k)}\mathbf{S}^{(k)}\mathbf{Dh}^{(k)}\right) \quad (12)\end{aligned}$$

where $\varepsilon^{(k)}$, $\mathbf{s}^{(k)}$, and $\mathbf{h}^{(k)}$ denote the (k)th estimates of ε, $\mathbf{s}$, and $\mathbf{h}$, respectively. Moreover, in (11) and (12), $\mathbf{R}^{(k)} = \mathbf{F}^H\mathbf{F}_{\upsilon^{(k)}}\mathbf{F} - \varepsilon^{(k)}\mathbf{I}$ where $\upsilon^{(k)} \approx (N/\pi(N-1))\Im\{\varepsilon^{(k)}\}$. It is seen that the expectation step of the proposed algorithm tries to separate and balance the desired signal and the interference signal so that any estimation error is properly allocated between them. Note that there is no need to evaluate $\mathbf{z}_I^{(k)}$ in (12), because the next maximization step employs only the desired signal $\mathbf{z}_D^{(k)}$ in (11).

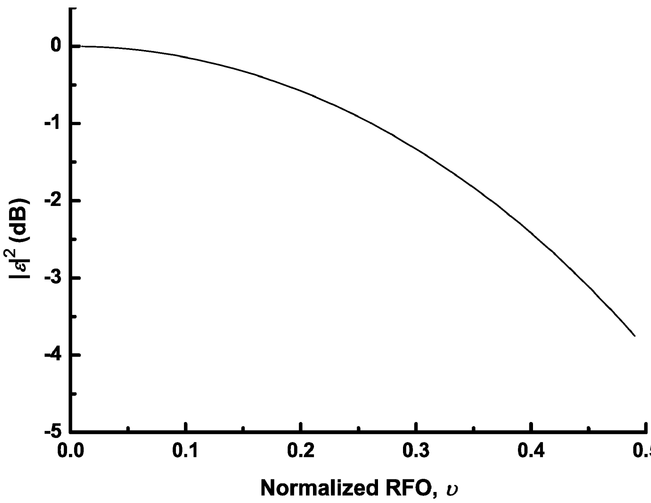

Fig. 1. Characterization of common RFO error ε according to the normalized RFO υ.

The maximization step at the (k)th iteration sequentially updates the parameter estimates [15] given by

$$\varepsilon^{(k+1)} = \underset{\varepsilon}{\operatorname{argmax}}\, \Lambda\left(\varepsilon, \mathbf{s}^{(k)}, \mathbf{h}^{(k)}|\mathbf{z}_D^{(k)}\right) \tag{13}$$

$$\upsilon^{(k+1)} \approx \frac{N}{\pi(N-1)}\Im\left\{\varepsilon^{(k+1)}\right\} \tag{14}$$

$$\mathbf{s}^{(k+1)} = \underset{\mathbf{s}}{\operatorname{argmax}}\, \Lambda\left(\varepsilon^{(k+1)}, \mathbf{s}, \mathbf{h}^{(k)}|\mathbf{z}_D^{(k)}\right) \tag{15}$$

$$\mathbf{h}^{(k+1)} = \underset{\mathbf{h}}{\operatorname{argmax}}\, \Lambda\left(\varepsilon^{(k+1)}, \mathbf{s}^{(k+1)}, \mathbf{h}|\mathbf{z}_D^{(k)}\right) \tag{16}$$

where the log-likelihood function $\Lambda(\varepsilon, \mathbf{s}, \mathbf{h}|\mathbf{z}_D)$ can be written as

$$\Lambda(\varepsilon, \mathbf{s}, \mathbf{h}|\mathbf{z}_D) = \Re\left\{\varepsilon \cdot \mathbf{z}_D^H\mathbf{SDh}\right\} - \frac{1}{2}|\varepsilon|^2|\mathbf{SDh}|^2. \tag{17}$$

Then, the solution of (13) can be evaluated as

$$\varepsilon^{(k+1)} = \frac{1}{\left|\mathbf{S}^{(k)}\mathbf{Dh}^{(k)}\right|^2}\left(\mathbf{S}^{(k)}\mathbf{Dh}^{(k)}\right)^H\mathbf{z}_D^{(k)}. \tag{18}$$

Moreover, assuming constant-envelope modulation schemes and applying the least-square (LS) solution, (16) results in

$$\mathbf{h}^{(k+1)} = \frac{\left(\varepsilon^{(k+1)}\right)^*}{\left|\varepsilon^{(k+1)}\right|^2}\mathbf{V}\left(\mathbf{S}^{(k)}\right)^H\mathbf{z}_D^{(k)} \tag{19}$$

where $\mathbf{V} = (\mathbf{D}^H\mathbf{D})^{-1}\mathbf{D}^H$. Note that $\beta_D = \beta_I = 1$ is the optimal condition to maximize the Fisher information of $\mathbf{z}_D$ and $\mathbf{z}_I$ in the SAGE algorithm [10], [15].

The proposed scheme employs only the desired signal $\mathbf{z}_D$ during the maximization step in (13)–(16), while the interference signal $\mathbf{z}_I$ also carries the information about the unknown parameters. Here, the proposed scheme may be considered as an approximate application of the SAGE algorithm or a suboptimal approach, which can be explained by the behavior of the common RFO error ε in (6). Fig. 1 shows the magnitude of the common RFO error ε as a function of the normalized RFO υ. The magnitude of ε decreases as the normalized RFO increases.

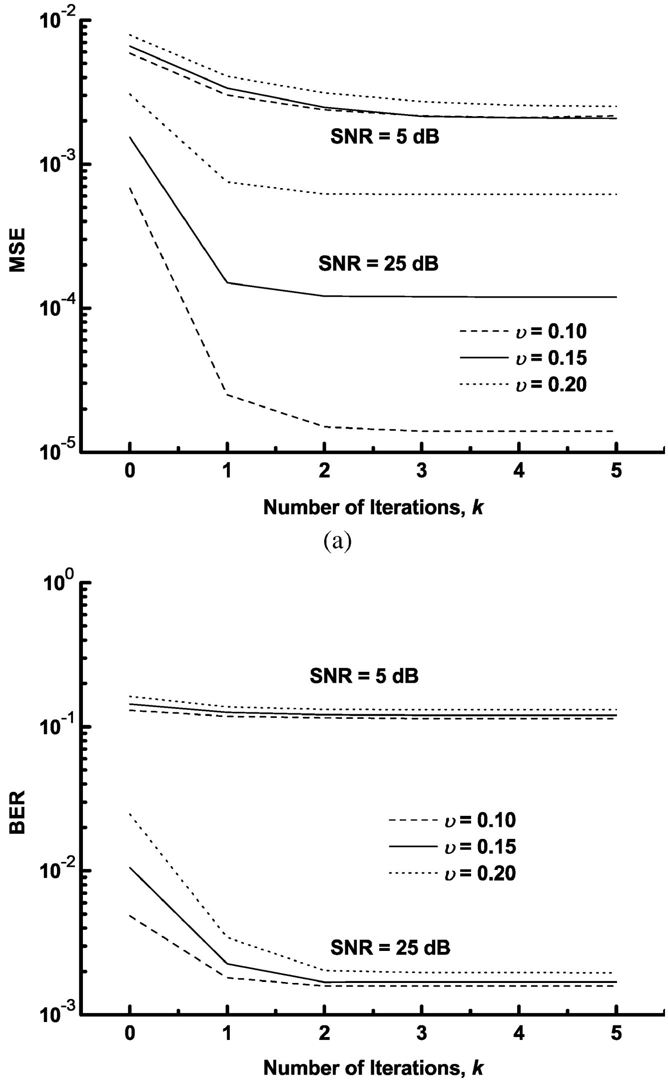

Fig. 2. Convergence properties of proposed algorithm. (a) MSE performance of RFO estimator. (b) BER performance.

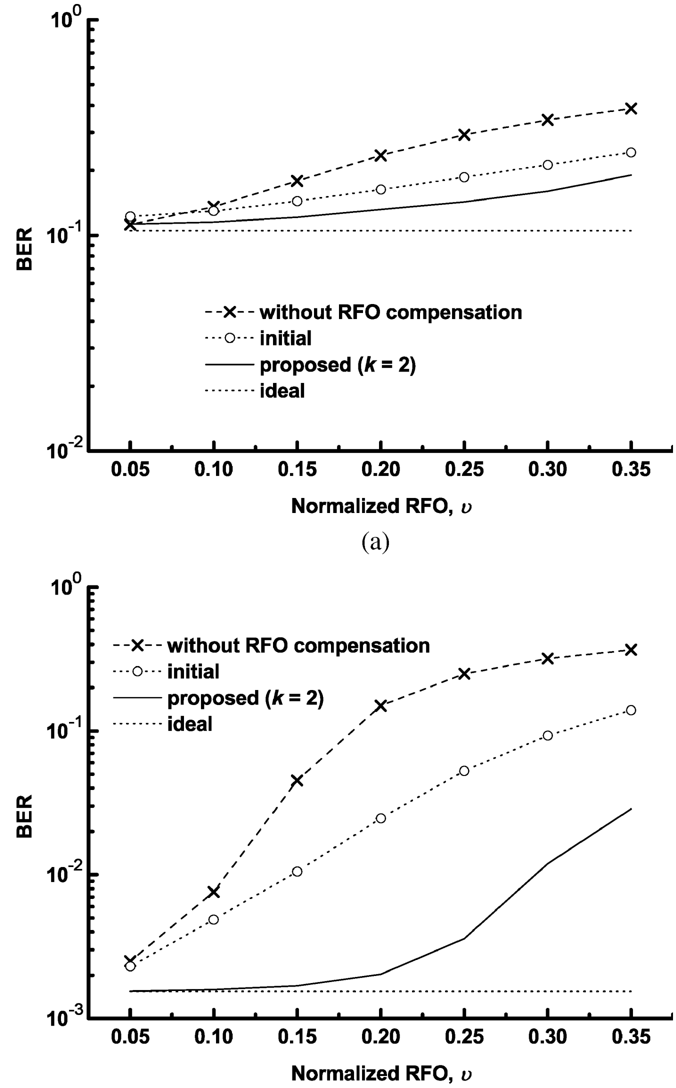

Fig. 3. Comparisons of BER performance according to the different values of normalized RFO υ. (a) SNR = 5 dB. (b) SNR = 25 dB.

The decreased $|\varepsilon|^2$ results in the reduction of the desired signal power as shown in (9), which is directly related to the increase of the interference signal power. Therefore, ignoring the interference signal $\mathbf{z}_I$, the proposed scheme may have the inherent loss as the normalized RFO increases.

B. Initialization

In order to begin the iteration, the initial estimates of ε, $\mathbf{s}$, and $\mathbf{h}$ are required. In the proposed scheme, the last CSI estimate $\mathbf{h}^{(k)}$ after k iterations at the previous OFDM symbol is used for the initial CSI estimate $\mathbf{h}^{(0)}$ at the current OFDM symbol, assuming that the channel variation between adjacent OFDM symbols is ignorable. For $\varepsilon^{(0)}$ and $\mathbf{s}^{(0)}$, however, the initial estimates should be evaluated using $\mathbf{z}$ in (5), including the ICI.

Let B pilots $\{s_b^{\text{pilot}}; 0 \le b < B\}$ be embedded in the OFDM symbol at known subcarrier locations $\{i_b; 0 \le b < B\}$ [11]. Here, we define $\mathbf{S}^{\text{pilot}} = \text{diag}\{s_0^{\text{pilot}}, s_1^{\text{pilot}}, \cdots, s_{B-1}^{\text{pilot}}\}$ and $[\mathbf{D}^{\text{pilot}}]_{b,l} = e^{-j(2\pi(i_b - N_\alpha)/N)l}$, where $b = 0, 1, \ldots, B-1$ and $l = 0, 1, \ldots, L-1$. Using pilot subcarriers and $\mathbf{h}^{(0)}$, the initial estimate $\varepsilon^{(0)}$ can be evaluated as

$$\varepsilon^{(0)} = \frac{1}{\left|\mathbf{S}^{\text{pilot}}\mathbf{D}^{\text{pilot}}\mathbf{h}^{(0)}\right|^2}\left(\mathbf{S}^{\text{pilot}}\mathbf{D}^{\text{pilot}}\mathbf{h}^{(0)}\right)^H \mathbf{z}^{\text{pilot}} \quad (20)$$

where $\mathbf{z}^{\text{pilot}} = [z^{\text{pilot}}(i_0)\; z^{\text{pilot}}(i_1) \; \cdots \; z^{\text{pilot}}(i_B - 1)]^T$. Then, given $\varepsilon^{(0)}$, we can obtain $\upsilon^{(0)} \approx (N/\pi(N-1))\Im\{\varepsilon^{(0)}\}$, as shown in (7). Using $\mathbf{h}^{(0)}$, $\varepsilon^{(0)}$, and the likelihood function in (17), the initial data-symbol estimate $\mathbf{s}^{(0)}$ can be evaluated by the following:

$$\mathbf{s}^{(0)} = \underset{\mathbf{s}}{\text{argmax}}\, \Lambda\left(\varepsilon^{(0)}, \mathbf{s}, \mathbf{h}^{(0)} | \mathbf{z}\right). \quad (21)$$

IV. Simulation Results

System parameters for our simulations follow IEEE 802.11a [16], and the subcarriers are modulated by quadrature phase-shift keying (QPSK). The fast Fourier transform (FFT) size and

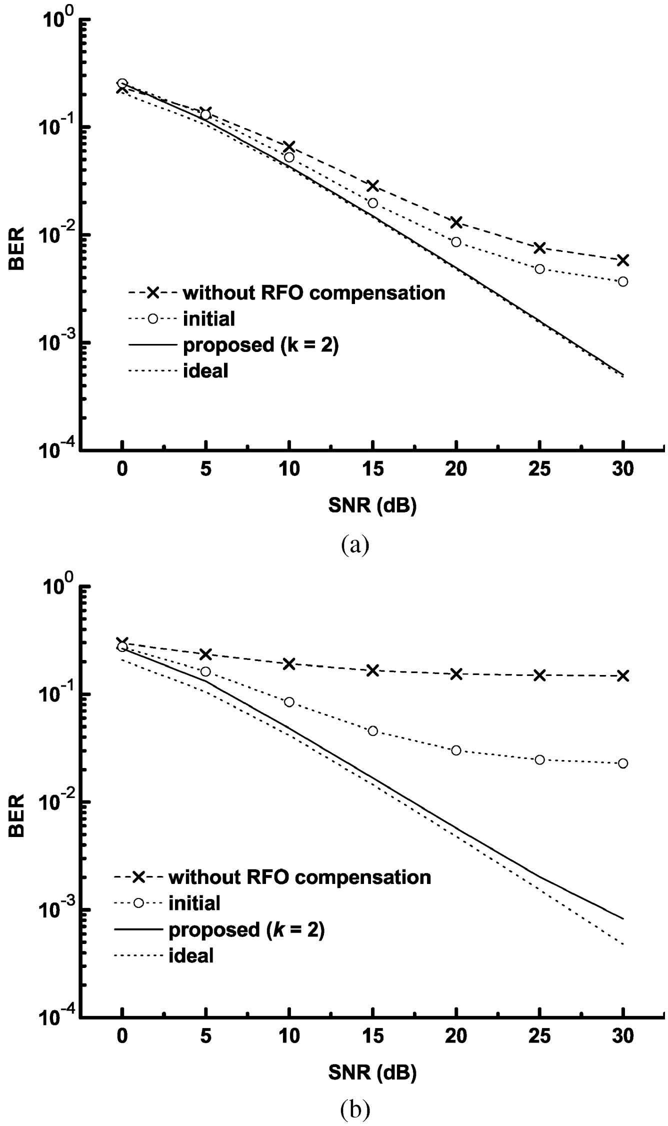

Fig. 4. BER versus SNR in time-varying channels. (a) $v = 0.1$. (b) $v = 0.2$.

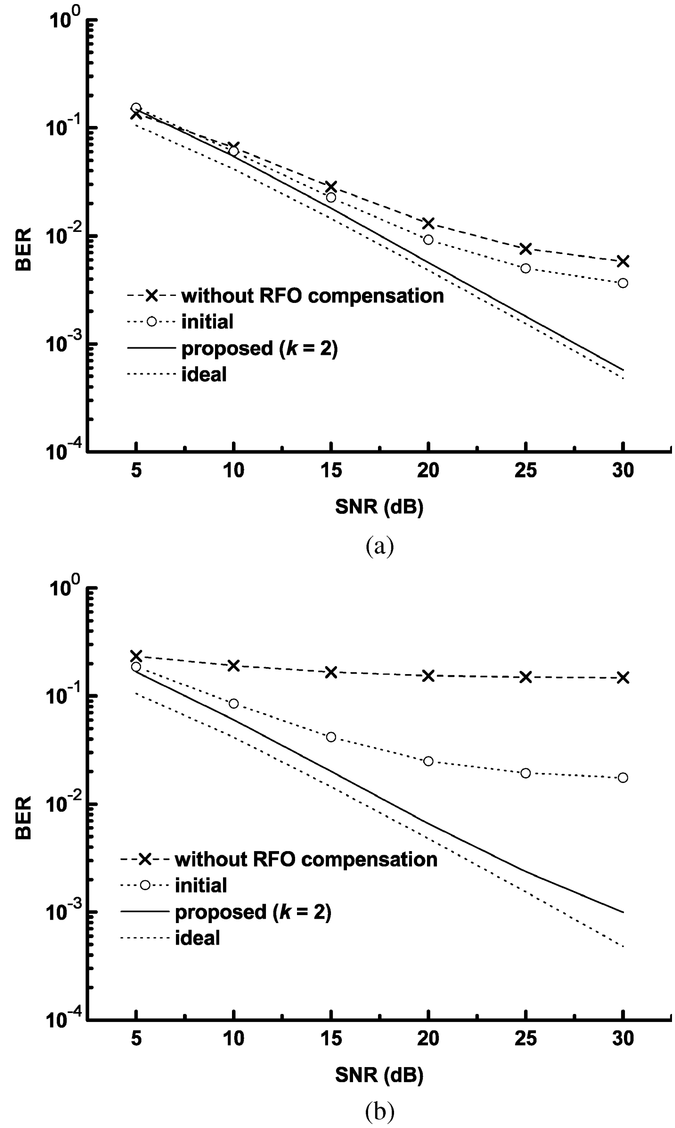

Fig. 5. BER versus SNR in static channels. (a) $v = 0.1$. (b) $v = 0.2$.

the number of modulated subcarriers are $N = 64$ and $N_s = 53$, respectively. The number of pilot subcarriers is $B = 4$. It is assumed that the power delay profile of the CIR is given by $E|h(l)|^2 \propto e^{-l/4}$, $0 \leq l < 8$, and each multipath varies according to Rayleigh distribution [17]. Moreover, one packet is composed of 100 OFDM symbols, and the first symbol of each packet is assigned as a preamble. It is assumed that the RFO is constant in each packet, and the RFO estimation process in (13) and (14) is performed only at the first OFDM data symbol after the preamble. The final estimate of the RFO is used at the other OFDM data symbols in the packet.

At first, we consider a static channel, which indicates that the channel is constant over a packet and the CSI is available at the receiver. Then, there is no need to include the CSI process in (16). Fig. 2 shows the convergence properties of the proposed algorithm. It is seen that two iterations are enough to obtain the converged mean-square error (MSE) and bit-error rate (BER) performance. Therefore, we fix the number of iterations to two in the following simulation results.

In Fig. 3, we present the BER performance of the proposed algorithm according to the different values of the normalized RFO v. It is also compared with the ideal performance in perfect synchronization, the performance without RFO compensation, and that of the initialization process described in Section III-B. We see that the proposed algorithm significantly compensates the performance degradation, especially at high signal-to-noise ratio (SNR), and it achieves almost ideal performance as long as $v < 0.2$. Fig. 4 presents the BER performance as a function of SNR. It is also seen that in all ranges of SNR, the proposed scheme achieves almost ideal performance, and remarkably compensates the performance degradation due to the RFO.

The following results show the BER performance of the proposed algorithm for a time-varying channel, which indicates that the channel variation should be tracked at each OFDM symbol. For our simulations, it is assumed that the carrier frequency and the vehicle speed are set to be 5 GHz and 60 km/h, respectively [17]. In this case, the proposed algorithm should include the CSI process in (16). Fig. 5 indicates that the degraded BER performance due to the RFO is also compensated significantly by the proposed scheme in time-varying channels.

V. Conclusion

In this letter, we propose an iterative RFO compensation scheme using the approximate application of the SAGE algorithm for OFDM systems. The expectation step in the proposed scheme extracts the desired terms from the received signals. Then, the maximization step is used to estimate the RFO, data symbols, and the CSI using the desired signal. Simulation results show that the proposed scheme needs two iterations to obtain converged estimates. Moreover, it significantly compensates the performance degradation due to the RFO and achieves almost ideal performance in all ranges of SNR, while the normalized RFO value is within 0.2.

Acknowledgment

The authors would like to thank the paper editor and the reviewers for their valuable comments and suggestions.

References

[1] M. Speth, S. A. Fechtel, G. Fock, and H. Meyr, "Optimum receiver design for wireless broadband systems using OFDM. I," *IEEE Trans. Commun.*, vol. 47, no. 11, pp. 1668–1677, Nov. 1999.

[2] F. Daffara and O. Adami, "A new frequency detector for orthogonal multicarrier transmission techniques," in *Proc. Veh. Technol. Conf.*, Jul. 1995, vol. 2, pp. 804–809.

[3] J. J. van de Beek, M. Sandell, and P. O. Borjesson, "ML estimation of timing and frequency offset in OFDM systems," *IEEE Trans. Signal Process.*, vol. 45, no. 7, pp. 1800–1805, Jul. 1997.

[4] T. M. Schmidl and D. C. Cox, "Robust frequency and timing synchronization for OFDM," *IEEE Trans. Commun.*, vol. 45, no. 12, pp. 1613–1621, Dec. 1997.

[5] A. J. Coulson, "Maximum-likelihood synchronization for OFDM using a pilot symbol: Algorithm," *IEEE J. Sel. Areas Commun.*, vol. 19, no. 12, pp. 2486–2494, Dec. 2001.

[6] F. Tufvesson, O. Edfors, and M. Faulkner, "Time and frequency synchronization for OFDM using PN-sequence preamble," in *Proc. Veh. Technol. Conf.*, Sep. 1999, vol. 4, pp. 2203–2207.

[7] X. Wang, T. T. Tjhung, Y. Wu, and B. Caron, "SER performance evaluation and optimization of OFDM system with residual frequency and timing offsets form imperfect synchronization," *IEEE Trans. Broadcast.*, vol. 49, no. 2, pp. 170–177, Jun. 2003.

[8] H. Lui and U. Tureli, "A high efficient carrier estimator for OFDM communications," *IEEE Commun. Lett.*, vol. 2, no. 4, pp. 104–106, Apr. 1998.

[9] S. Attallah, "Blind estimation of residual carrier offset in OFDM systems," *IEEE Signal Process. Lett.*, vol. 11, no. 2, pp. 216–219, Feb. 2004.

[10] J. A. Fessler and A. O. Hero, "Space-alternating generalized expectation-maximization algorithm," *IEEE Trans. Signal Process.*, vol. 42, no. 10, pp. 2664–2677, Oct. 1994.

[11] M. Morelli and U. Mengali, "A comparison of pilot-aided channel estimation methods for OFDM system," *IEEE Trans. Signal Process.*, vol. 49, no. 12, pp. 3065–3073, Dec. 2001.

[12] M. Feder and E. Weinstein, "Parameter estimation of superimposed signals using the EM algorithm," *IEEE Trans. Acoust., Speech, Signal Process.*, vol. 36, no. 4, pp. 477–489, Apr. 1988.

[13] C. N. Georghiades and J. C. Han, "Sequence estimation in the presence of random parameters via the EM algorithm," *IEEE Trans. Commun.*, vol. 45, no. 3, pp. 300–308, Mar. 1997.

[14] Y. Xie and C. N. Georghiades, "Two EM-type channel estimation algorithms for OFDM with transmitter diversity," *IEEE Trans. Commun.*, vol. 51, no. 1, pp. 106–115, Jan. 2003.

[15] B. H. Fleury, M. Tschudin, R. Heddergott, D. Dahlhaus, and K. I. Pedersen, "Channel parameter estimation in mobile radio environments using SAGE algorithm," *IEEE J. Sel. Areas Commun.*, vol. 17, no. 3, pp. 434–450, Mar. 1999.

[16] *Part 11: "Wireless LAN Medium Access Control (MAC) and Physical Layer (PHY) Specifications: High-speed Physical Layer in the 5 GHz Band"*, IEEE 802.11 WG, Sep. 1999, Supplement to IEEE 802.11.

[17] W. C. Y. Lee, *Mobile Communications Engineering*. New York: McGraw-Hill, 1982.